

Curvilinear coordinate Generalized Source Method for gratings having continuous piecewise-smooth profiles

Alexey A. Shcherbakov^{1,2}

¹ITMO University

²Moscow Institute of Physics and Technology

April 12, 2019

Abstract

High-efficient direct numerical methods are currently in demand for optimization procedures in the fields of both conventional diffractive and metasurface optics. With a view of extending the scope of application of the previously proposed Generalized Source Method in the curvilinear coordinates having $O(N \log N)$ asymptotic numerical complexity a new method formulation is developed for gratings having continuous non-smooth corrugation profiles. It is shown that corrugation corners can be treated as effective medium interfaces within the rationale of the method. Moreover, the given formulation is demonstrated to allow for application of the same derivation as one used in classical electrodynamics to derive the interface conditions. This yields continuous combinations of the fields and metric tensor components, which can be directly Fourier factorized. Together with an efficient algorithm the new formulation is demonstrated to substantially increase the computation accuracy for given computer resources.

1 Introduction

Electromagnetic planar grating diffraction problem for resonant domain structures composed of dispersive materials can be solved by various numerical methods depending on particular structure properties [1, 2]. While the direct diffraction problem often is not an issue in practice, related inverse problems impose strict requirements on the mentioned methods as a huge number of direct problem simulation runs is generally required within inversion procedures [3]. This makes the research directed towards the increase of simulation efficiency in terms of computing resource requirements be in demand in the field of engineering of high-efficient optical structures, like resonant gratings [4]. In particular, efficient optimization procedures are of great interest within the modern trend of metasurface optimization, which is aimed at pushing forward the field so as to substitute conventional diffractive optical components with high-index metastructures.

Fourier space methods are good candidates for the purpose of large scale optimization of periodic dielectric structures being versatile in terms of structure geometries and offering a reliable convergence error analysis [5, 6]. There were proposed several fast numerical schemes exhibiting an $O(N \log N)$ numerical complexity and $O(N)$ computational memory resort [7, 8, 9, 10, 11],

and providing a large room for parallelization on vector processors. Owing to these features the named methods possess a great potential for applications in optimization procedures, though some additional specific improvements are required to ensure convergence for complex diffractive optical elements and metasurfaces. These improvements include the scattering vector algorithm [12], which implements the divide-and-conquer strategy for thick structures, and application of curvilinear coordinate transformations, which improve the numerical behavior of the Fourier methods. These transformations are of two types. The first type implies in-plane stretching and contracting a grating, and was developed within the context of the Fourier Modal Method (FMM) [13, 14, 15] and the Modal Method (MM) [16, 17] to simplify the correct treatment of the boundary conditions [18, 19, 20] and improve numerical solution conditioning. A similar procedure can be incorporated into the fast methods, though this possibility is not considered in this work. The second type of transformations, which inevitably affects the coordinate orthogonal to the grating plane, includes transformations converting a complex corrugation interface to a plane. An idea of such transformations gave rise to the Chandezon method [21, 22, 23] being an analog of the FMM in the curvilinear coordinate space. In [24, 25] this idea was expanded to fit the rationale of computationally efficient methods by introducing the generalized metric sources. The corresponding method will be referred to as the Generalized Source Method in Curvilinear Coordinates (GSMCC), and its implementation paved a way to the efficient Fourier space simulation of metallic structures. However, the formulation given in [24, 25] is based on an assumption of the smoothness of functions describing periodic corrugations, thus, having a limited range of validity. In this work a generalization of the latter methods is developed in case of 1D gratings, which profile functions are allowed to have discontinuous derivatives.

The article structure is the following. The narrative starts with the grating diffraction problem statement. Then the GSMCC rationale is outlined in form of a sequence of steps leading to a required solution form. Details on the corresponding derivations can be found in the previous papers [24, 25, 26]. A consequent analysis of effective metric sources and the Maxwell's equations in curvilinear metric yields the derivation of correct handling of truncated Fourier vectors. Next, an efficient numerical method based on these rules is described. Numerical examples and the discussion of the results enclose the paper.

2 Grating diffraction

Let us consider a simple case of a periodic grating corrugation separating two different media, which is supposed to be described by a continuous piecewise-smooth periodic function $x_3 = f(x_1)$, with period Λ , such that $f(x_1 + n\Lambda) = f(x_1)$, $n \in \mathbb{N}$, in the Cartesian coordinates x_α , $\alpha = 1, 2, 3$. Without loss of generality one can suppose that $\min f(x_3) = -a$, $\max f(x_3) = a$. Dielectric permittivities of the media below and above the corrugation interface are denoted as ε_1 and ε_2 respectively. Fig. 1(a) illustrates the setup. Linear electromagnetic optical diffraction is governed by the time-harmonic Maxwell's equations with implicit time dependence factor $\exp(-i\omega t)$

$$\begin{aligned}\xi_{\alpha\beta\gamma}\partial_\beta E_\gamma(\mathbf{r}) &= i\omega\mu_0 H_\alpha(\mathbf{r}) - M_\alpha(\mathbf{r}), \\ \xi_{\alpha\beta\gamma}\partial_\beta H_\gamma(\mathbf{r}) &= -i\omega\varepsilon(\mathbf{r}) E_\alpha(\mathbf{r}) + J_\alpha(\mathbf{r})\end{aligned}\tag{1}$$

subject to the continuity of the tangential fields at the corrugation interface, and the radiation condition at $x_3 \rightarrow \pm\infty$ [2]. Here $\xi_{\alpha\beta\gamma}$ is the Levi-Civita symbol, Greek indices vary in range 1, 2, 3,

and $\mathbf{r} = (x_1, x_2, x_3)^T$. Summation over repeated coordinate indices is supposed here and further. Permittivity function is $\varepsilon(\mathbf{r}) = \varepsilon_1$ when $x_3 \leq f(x_1)$, and $\varepsilon(\mathbf{r}) = \varepsilon_2$ when $x_3 > f(x_1)$.

To set up a general solution of Eqs. (1), first, the dielectric permittivity and the magnetic permeability inside some region $D_g = \{|x_3| \leq b : b \geq a\}$ incorporating the grating are assumed to be constant everywhere $\varepsilon(\mathbf{r}) = \varepsilon_b$, $\mu = \mu_b$, with the subscript standing for ‘‘basis’’. This assumption replaces the grating with a homogeneous plane layer. The electromagnetic field for this basis layer can be found for any sources by the volume integral equations with the electric and magnetic Green’s tensors $G_{\alpha\beta}^{E,M}(\mathbf{r}, \mathbf{r}')$. Attributing the ‘‘difference’’ between the grating and the layer to effective (generalized) sources, one attains a self-consistent linear equation system for the searched solution of the diffraction problem. For the planar grating problem the Green’s tensors are subject to the plane wave decomposition (see, e.g., [27, 26]). In order to get rid of a singular term proportional to $\delta(x_3 - x'_3)$ present in the explicit form of $G_{\alpha\beta}^E(\mathbf{r}, \mathbf{r}')$ it is convenient to introduce the modified fields as $\tilde{E}_3 = E_3 - J_3/i\omega\varepsilon_b$, $\tilde{H}_3 = H_3 - M_3/i\omega\mu_b$, with the rest components being untouched: $\tilde{E}_{1,2} = E_{1,2}$, $\tilde{H}_{1,2} = H_{1,2}$. The periodicity allows one to fix a zero harmonic wave vector $\mathbf{k}^{inc} = (k_1^{inc}, 0, k_3^{inc})$ and to represent the fields and sources in form of Bloch waves. This makes possible a decomposition of the modified electromagnetic field into a set of TE (superscript ‘‘e’’) and TM (superscript ‘‘h’’) polarized plane waves propagating upwards and downwards relative to the vertical coordinate x_3 :

$$\tilde{E}_\alpha(\mathbf{r}) = \sum_{m=-\infty}^{\infty} \sum_{\sigma=\pm} [\tilde{a}_m^{e\sigma}(x_3) \hat{e}_{m\alpha}^{e\sigma} + \tilde{a}_m^{h\sigma}(x_3) \hat{e}_m^{h\sigma}] \exp(ik_{m1}x_1 + i\sigma k_{m3}x_3), \quad (2)$$

$$\tilde{H}_\alpha(\mathbf{r}) = \frac{k_b}{\omega\mu_0} \sum_{m=-\infty}^{\infty} \sum_{\sigma=\pm} [\tilde{a}_m^{h\sigma}(x_3) \hat{e}_{m\alpha}^{e\sigma} - \tilde{a}_m^{e\sigma}(x_3) \hat{e}_m^{h\sigma}] \exp(ik_{m1}x_1 + i\sigma k_{m3}x_3), \quad (3)$$

where the index m enumerates a discrete set of plane waves having wavevectors $\mathbf{k}_m^\pm = (k_{m1}, 0, \pm k_{m3})$ defined by the grating equation $k_{m1} = k_1^{inc} + 2\pi m/\Lambda$, and the dispersion equation $k_{m1}^2 + k_{m3}^2 = k_b^2$, $\Re k_{m3} + \Im k_{m3} \geq 0$ with $k_b = \omega\sqrt{\varepsilon_b\mu_0}$. Unit vectors $\hat{e}_m^{e\pm}$ and $\hat{e}_m^{h\pm}$, which specify the polarization, explicitly write

$$\begin{aligned} \hat{e}_m^{e\pm} &= \frac{\mathbf{k}_m^\pm \times \hat{e}_3}{|\mathbf{k}_m^\pm \times \hat{e}_3|}, \\ \hat{e}_m^{h\pm} &= \frac{(\mathbf{k}_m^\pm \times \hat{e}_3) \times \mathbf{k}_m^\pm}{|(\mathbf{k}_m^\pm \times \hat{e}_3) \times \mathbf{k}_m^\pm|}. \end{aligned} \quad (4)$$

The vertical coordinate dependent amplitudes occurring in Eqs. (2), (3) are solutions of the following integral equations (see [26] for a detailed derivation)

$$\tilde{a}_m^{e+}(x_3) = \tilde{a}_m^{ext,e+}(x_3) - \int_{-\infty}^{x_3} d\zeta \frac{\mathcal{G}_m(x_3, \zeta)}{2k_{m3}} [\omega\mu_b \hat{e}_m^{e+} \cdot \mathbf{J}_m(\zeta) - k_b \hat{e}_m^{h+} \cdot \mathbf{M}_m(\zeta)], \quad (5)$$

$$\tilde{a}_m^{h+}(x_3) = \tilde{a}_m^{ext,h+}(x_3) - \int_{-\infty}^{x_3} d\zeta \frac{\mathcal{G}_m(x_3, \zeta)}{2k_{m3}} [\omega\mu_b \hat{e}_m^{h+} \cdot \mathbf{J}_m(\zeta) + k_b \hat{e}_m^{e+} \cdot \mathbf{M}_m(\zeta)], \quad (6)$$

$$\tilde{a}_m^{e-}(x_3) = \tilde{a}_m^{ext,e-}(x_3) - \int_{x_3}^{\infty} d\zeta \frac{\mathcal{G}_m(x_3, \zeta)}{2k_{m3}} [\omega\mu_b \hat{e}_m^{e-} \cdot \mathbf{J}_m(\zeta) - k_b \hat{e}_m^{h-} \cdot \mathbf{M}_m(\zeta)], \quad (7)$$

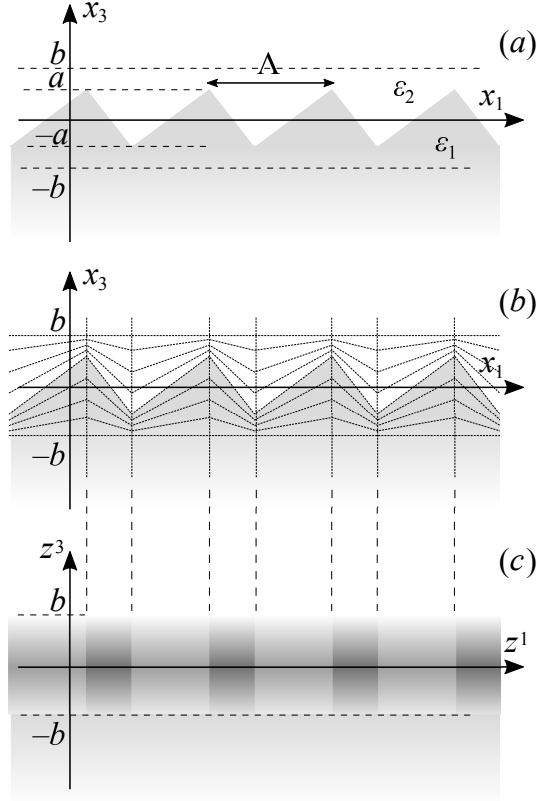


Figure 1: (a) Grating of period Λ , depth $2a$, and the grating region $D_g = \{|x_3| \leq b : b \geq a\}$; (b) isolines of the curvilinear coordinates, which contain a plane coinciding with the corrugation interface, and continuously become the Cartesian at $x_3 = \pm b$ boundaries; (c) illustration of an effective periodic structure which can be thought to give rise to the generalized metric sources; the structure has sharp vertical interfaces when the grating corrugation profile has corners.

$$\tilde{a}_m^{h-}(x_3) = \tilde{a}_m^{ext,h-}(x_3) - \int_{x_3}^{\infty} d\zeta \frac{\mathcal{G}_m(x_3, \zeta)}{2k_{m3}} [\omega \mu_b \hat{\mathbf{e}}_m^{h-} \cdot \mathbf{J}_m(\zeta) + k_b \hat{\mathbf{e}}_m^{e-} \cdot \mathbf{M}_m(\zeta)], \quad (8)$$

with the coefficients $\mathcal{G}_m(\xi, \eta)$ coming from the plane wave decomposition of the Green's tensor. In general case of a planar waveguide they can be found, e.g., in [25, 28], and in particular, when $\epsilon_b = \epsilon_1 = \epsilon_2$ they explicitly read $\mathcal{G}_m(\xi, \eta) = \exp(ik_{3m}|\xi - \eta|)$. Here it is supposed that the sources are split in two parts: the first part excites some known external fields $E_\alpha^{ext}, H_\alpha^{ext}$ with plane wave decomposition amplitudes $\tilde{a}_m^{ext,e,h\pm}(x_3)$, while the second part J_α, M_α present in the integrands correspond to some local sources to be specified below, which bring an information about the mentioned difference between the grating and the plane homogeneous layer in the region D_g .

3 Generalized metric sources

Once the general solution equations (5)-(8) are established they can be enclosed on the basis of the curvilinear coordinate transformation idea mentioned in the introduction. Consider curvilinear coordinates (z^1, z^2, z^3) such that in $D_g = \{|x_3| \leq b : b \geq a\}$ the coordinate plane $z^3 = 0$ coincides

with the corrugation profile, and the coordinates continuously become Cartesian at boundaries $\partial D = \{x_3 = \pm b\}$. Such transformation can be defined as

$$\begin{aligned} x_{1,2} &= z^{1,2}, \\ x_3 &= \begin{cases} z^3 + \mathcal{F}(z^3) f(z^1), & |x_3| \leq b \\ z^3, & |x_3| > b \end{cases} \end{aligned} \quad (9)$$

where $\mathcal{F}(z^3) = 1 - |z^3|/b$. An illustrative example is given in Fig. 1(b). Possible generalizations of the definition (9) concern multilayer structures, and are discussed in [25] with the difference that the corrugation function $f(x_1)$ is not required to be smooth here. Transformation (9) yields the metric tensor

$$\{g^{\alpha\beta}\} = \begin{pmatrix} 1 & 0 & -\frac{\mathcal{F}f'}{(1+\mathcal{F}'f)^2} \\ 0 & 1 & 0 \\ -\frac{\mathcal{F}f'}{(1+\mathcal{F}'f)^2} & 0 & \frac{1+\mathcal{F}^2f'^2}{(1+\mathcal{F}'f)^2} \end{pmatrix}, \quad (10)$$

which components are discontinuous functions of coordinates due to discontinuity of the derivative f' .

Being written in the curvilinear coordinates the Maxwell's equations become [29]

$$\begin{aligned} \xi^{\alpha\beta\gamma} \partial_\beta E_\gamma(\mathbf{r}) &= i\omega\mu_0 \sqrt{g} g^{\alpha\beta} H_\beta(\mathbf{r}) - M^\alpha(\mathbf{r}) \\ \xi^{\alpha\beta\gamma} \partial_\beta H_\gamma(\mathbf{r}) &= -i\omega\varepsilon(\mathbf{r}) \sqrt{g} g^{\alpha\beta} E_\beta(\mathbf{r}) + J^\alpha(\mathbf{r}) \end{aligned} \quad (11)$$

where the lower and upper indices distinguish the covariant and contravariant vector components respectively, and g denotes the determinant of a matrix being inverse to (10): $g = \det\{g_{\alpha\beta}\} = 1/\det\{g^{\alpha\beta}\}$. An observation that the metric tensor explicitly occurs only behind the field terms in the right-hand parts of Eq. (11) brings the second cornerstone idea of the GSMCC [24]: Eqs. (11) can be rewritten in a form similar to the Maxwell's equations in the Cartesian coordinates (1) and the rest can be attributed to generalized electromagnetic sources originating from the difference between the curvilinear and Cartesian coordinates. Namely, Eqs. (11) become

$$\begin{aligned} \xi^{\alpha\beta\gamma} \partial_\beta E_\gamma(\mathbf{r}) &= i\omega\mu_b \delta^{\alpha\beta} H_\beta(\mathbf{r}) - M_{gen}^\alpha(\mathbf{r}) - M^\alpha(\mathbf{r}), \\ \xi^{\alpha\beta\gamma} \partial_\beta H_\gamma(\mathbf{r}) &= -i\omega\varepsilon_b \delta^{\alpha\beta} E_\beta(\mathbf{r}) + J_{gen}^\alpha(\mathbf{r}) + J^\alpha(\mathbf{r}) \end{aligned} \quad (12)$$

with the generalized metric sources

$$\begin{aligned} J_{gen}^\alpha(\mathbf{r}) &= -i\omega\varepsilon_b (\eta_e \sqrt{g} g^{\alpha\beta} - \delta^{\alpha\beta}) E_\beta(\mathbf{r}), \\ M_{gen}^\alpha(\mathbf{r}) &= -i\omega\mu_b (\eta_h \sqrt{g} g^{\alpha\beta} - \delta^{\alpha\beta}) H_\beta(\mathbf{r}). \end{aligned} \quad (13)$$

Here $\eta_e = \varepsilon(\mathbf{r})/\varepsilon_b$, $\eta_h = \mu_0/\mu_b$. Due to the similarity between the operator parts of Eqs. (1) and Eqs. (12) such decomposition allows directly using solutions (5)-(8) with the sources (13) upon a direct substitution of the coordinates x_α with z^α and recalling that the modified fields should replace the real ones in Eq. (13). The function $\varepsilon(\mathbf{r})$ in the latter equations depends only on the coordinate z^3 and takes two constant values below and above the flattened corrugation interface: $\varepsilon(\mathbf{r}) = \varepsilon_1$ for $z^3 \leq 0$, and $\varepsilon(\mathbf{r}) = \varepsilon_2$ for $z^3 > 0$, in accordance with the definition of Eq. (9).

In analogy with the Generalized Source Method [7, 9] and other volume integral methods in the Fourier space, which enclose the volume integral equation with sources of the form $\mathbf{J} =$

$-i\omega [\varepsilon(\mathbf{r}) - \varepsilon_b] \mathbf{E}$, Eq. (13) demonstrates that the curvilinear metric impact can be treated as inhomogeneous and anisotropic material tensors $\hat{\varepsilon}^{\alpha\beta} = \varepsilon(\mathbf{r}) \sqrt{g} g^{\alpha\beta}$, and $\hat{\mu}^{\alpha\beta} = \mu_b \sqrt{g} g^{\alpha\beta}$. Due to the discontinuity of the metric tensor along the coordinate z^1 the points of discontinuity appear to effectively act like vertical material interfaces, as Fig. 1(c) illustrates. Thus, special precautions should be taken when calculating Fourier coefficients of the generalized metric sources to be used in Eqs. (5)-(8), in analogy with the Fourier methods in the Cartesian space [18]. In case of the C-method the factorization rules were thoroughly explained in [30] in terms of relations between covariant field components. The same rationale can be applied to the GSMCC, though, here the correct Fourier space matrix-vector relations are demonstrated to appear in a way analogous to the derivation of the electromagnetic interface conditions, as the following section explains.

4 Fourier factorization of discontinuous metric sources

In order to demonstrate the correct truncated Fourier factorization of the generalized metric sources consider the Maxwell's equations for the TE polarization (due to the presence of the both electric and magnetic sources derivations for the TM polarization are quite similar):

$$\begin{aligned} \partial_3 E_2 &= M^1 - i\omega \mu_b H_1, \\ \partial_1 E_2 &= -M^3 + i\omega \mu_b H_3, \\ \partial_3 H_1 - \partial_1 H_3 &= -i\omega \varepsilon_b E_2 + J^2, \end{aligned} \tag{14}$$

where the source terms represent a superposition of real sources exciting incoming diffracting waves, and the local generalized metric sources. In addition to Eqs. (14) let us explicitly recall the Gauss law

$$\begin{aligned} \partial_1 [\sqrt{g} (H_1 + g^{13} H_3)] + \partial_3 [\sqrt{g} (g^{31} H_1 + g^{33} H_3)] &= 0, \\ \partial_2 (\sqrt{g} E_2) &= 0. \end{aligned} \tag{15}$$

Here an independency of $\varepsilon(\mathbf{r})$ from the coordinates $z^{1,2}$ and $g^{11} = 1$ property of Eq. (10) are taken into account. The existence of the right-hand parts of Eqs. (14), (15) requires the existence of corresponding derivatives. Recalling the transition to the modified field and Eqs. (13), the last of Eq. (14), and the first of Eq. (15) become

$$\begin{aligned} \partial_3 \tilde{H}_1 - \partial_1 C_2 &= -i\omega \varepsilon_b \tilde{E}_2 + J^2, \\ \partial_1 C_1 + \partial_3 \tilde{H}_3 &= 0, \end{aligned} \tag{16}$$

where the non-trivial combinations of the field and the metric tensor components

$$\begin{aligned} C_1 &= \frac{1}{\sqrt{g} g^{33}} \tilde{H}_1 + \frac{g^{13}}{g^{33}} \frac{1}{\eta_h} \tilde{H}_3 \\ C_2 &= -\frac{g^{31}}{g^{33}} \tilde{H}_1 + \frac{1}{\sqrt{g} g^{33}} \frac{1}{\eta_h} \tilde{H}_3 \end{aligned} \tag{17}$$

should be continuous along z^1 coordinate, and, hence, across the effective vertical interfaces discussed at the end of the previous section. The continuity property follows directly from the same

derivations as the ones widely used in university textbooks to attain the electromagnetic interface conditions, (e.g. [31], Ch. 1.5.). Substitution of the explicit $g^{\alpha\beta}$ components into Eq. (17) yields

$$\begin{aligned} (\mathcal{F}f') C_1 - C_2 &= -(1 + \mathcal{F}'f) \frac{1}{\eta_b} \tilde{H}_3 \\ C_1 + (\mathcal{F}f') C_2 &= (1 + \mathcal{F}'f) \tilde{H}_1 \end{aligned} \quad (18)$$

Due to the continuity of $C_{1,2}$ and $1 + \mathcal{F}'f$ along z^1 one can take the Fourier transform of the latter equations [18] to derive relations between the Fourier coefficients $C_{1,2m}$ and $\tilde{H}_{1,3m}$. Denoting the Fourier component vectors with square brackets as $[\bullet]$, Fourier-Toeplitz matrices with double square brackets as $[[\bullet]]$, expressing explicitly $[C_{1,2}]$ via $[[\tilde{H}_{1,3}]]$, and substituting the modified fields into Eq. (13) one attains the following expressions for the Fourier components of the generalized metric sources:

$$[J^2] = -i\omega\varepsilon_b (\eta_e \mathcal{A} - \mathcal{I}) [\tilde{E}_2], \quad (19)$$

$$\begin{pmatrix} [M^1] \\ [M^3] \end{pmatrix} = -i\omega\mu_b \begin{pmatrix} \eta_h [C_1] - [\tilde{H}_1] \\ [\tilde{H}_3] - [C_2] \end{pmatrix} = -i\omega\mu_b (\mathcal{I} + \mathcal{B}\mathcal{B})^{-1} \begin{pmatrix} \eta_h \mathcal{I} & -\mathcal{B} \\ \mathcal{B} & \frac{1}{\eta_h} \mathcal{I} \end{pmatrix} \mathcal{A} \begin{pmatrix} [\tilde{H}_1] \\ [\tilde{H}_3] \end{pmatrix}, \quad (20)$$

where matrices $\mathcal{A} = [[1 + \mathcal{F}'f]]$, $\mathcal{B} = [[\mathcal{F}f']]$, and \mathcal{I} is the identity matrix. These equations hold for each fixed value of z^3 .

5 Numerical method

Definition of the coordinate transformation, Eq. (9), implies that the generalized metric sources (13) are non-zero only when $|z^3| \leq b$. Therefore, the integration limits in Eqs. (5)-(8) do not fall outside the region D_g . Let us introduce an equidistant mesh (slicing) in D_g defined by coordinates $z_k^3 = (2k + 1 - N_s) b / N_s$, $k = 0, \dots, N_s - 1$, with slice thickness $h_s = 2b / N_s$, and evaluate the integrals at the mesh points using the mid-point rule.

To attain a self-consistent linear equation system one has to truncate the infinite Fourier vectors and matrices to a maximum order N_F . It is convenient to solve the matrix equation on unknown vector $\{\mathcal{F}^e\}_{mk} = \left(\tilde{E}_{m2}(z_k^3), \tilde{H}_{m1}(z_k^3), \tilde{H}_{m3}(z_k^3) \right)^T$ (in case of the TE polarization) containing the Fourier amplitudes of the field components in each slice such that the Fourier index m runs in range $-N_F \leq m \leq N_F$ and the spatial mesh index k – in range $0 \leq k < N_s$. Eqs. (5)-(8) reduce to a set of linear equations on the unknown block vector of the TE wave amplitudes in each slice $\mathbf{a}_{mk}^e = (\tilde{a}_m^{e+}(z_k^3), \tilde{a}_m^{e-}(z_k^3))^T$:

$$\mathbf{a}^e = \mathbf{a}^{e,ext} + \mathbf{G}\mathbf{P}^e\Omega^e\mathbf{M}^{-1}\mathbf{N}\epsilon^e\mathcal{F}^e. \quad (21)$$

Here $\mathbf{a}^{e,ext}$ is the known amplitude vector of waves coming from the exterior of the layer D_g . This reduction is analogous to what is done in [24, 25], but here one faces with an additional matrix inversion present in Eq. (20). To handle this inversion the field-to-source transformation given by Eqs. (19), (20) is split into three matrices \mathbf{N} , \mathbf{M} and Ω^e . The matrix \mathbf{P}^e defines the source-to-amplitude in-slice transformation of Eqs. (5)-(8); and matrix \mathbf{G} is defined by operator \mathcal{G} . Additionally, the diagonal matrix $\epsilon^e : \{\epsilon^e\}_{mn,kl} = \delta_{mn}\delta_{kl} \text{diag} \{ \varepsilon_b, \mu_b, \mu_b \}$ shows the corresponding

scalar factors of Eqs. (19), (20), whereas the factor $-i\omega h_s/2$ is implicitly included in G . Explicitly all these matrices are written out in the Appendix. To solve for unknown field amplitudes one additionally has to pass from TE amplitudes to the field component amplitudes as $\mathcal{F}^e = Q^e \mathbf{a}^e$, where Q^e is composed of components of Eq. (4). This yields after some algebra

$$\mathcal{J}^e = M^{-1} N \epsilon^e \mathcal{F}^e = (M - N Q^e G P^e \Omega)^{-1} N \epsilon^e \mathcal{F}^{e,ext}. \quad (22)$$

The latter system is solved for the unknown vector \mathcal{J}^e , this vector can be substituted into Eq. (21) to attain the diffracted amplitude vector at the grating region boundaries:

$$\mathbf{a}^{e,out} = \mathbf{a}_b^{e,ext} + G_b Q^e \Omega^e \mathcal{J}^e \quad (23)$$

where the output and external amplitude vectors at grating region boundaries are $\left\{ \mathbf{a}_b^{e,out/ext} \right\}_m = \left(\tilde{a}_m^{out/ext,e+}(b), \tilde{a}_m^{e-}(-b) \right)^T$, and the matrix operator G_b also comes from tensor \mathcal{G} , and ‘‘collects’’ the waves diffracted in each slice at D_g boundaries. Since the curvilinear metric continuously transforms to the Cartesian one at $|z^3| = b$, and the modified field coincides with the real one outside the grating region, the output amplitudes immediately define the diffracted field outside D_g , and no other transformation is required.

The provided formulation of Eqs. (22), (23) preserves the fast and memory efficient conception of the previous papers [24, 25], and allows one to perform the grating diffraction calculation in $O(N \log N)$ time and $O(N)$ memory resort with $N = N_s N_F$. Namely, multiplications by block-diagonal matrices P^e , Q^e , G , and G_b are of linear asymptotic complexity, and multiplications by N , M , and Ω^e are of $O(N \log N)$ asymptotic complexity due to the block-Toeplitz structure.

Examples of the method convergence in dependence of N_F are given in Figs. 2,3 for an isoscales triangular corrugation profile analyzed with the formulation of [24], which is incorrect for grating with corners, and with the correct formulation provided here. Grating depth-to-wavelength ratio is taken to be $2a/\lambda = 0.5$, and the period-to-wavelength ratio – to be $\Lambda/\lambda = 1.5$ with the angle of incidence being 10° . The number of slices was taken to be $N_s = 512$. Fig. 2 corresponds to the dielectric grating with $\epsilon_1 = 1$, $\epsilon_2 = (2.5)^2$, whereas Fig. 3 corresponds to the metallic grating with the same ϵ_1 and $\epsilon_2 = (0.2 + 3.2i)^2$. The lower pairs of graphs in each figure demonstrate the convergence of the central part of diffraction amplitude vector $\mathbf{a}^{e,out}$ corresponding to the lowest used number of Fourier harmonics, namely $N_{F,min} = 8$ for the dielectric grating, and $N_{F,min} = 16$ for the metallic grating. The graphs demonstrate the superior accuracy and the rate of convergence in case of the correct formulation.

6 Conclusion

To summarize this work extends the applicability of the GSMCC method by providing an explicit formulation of the method in case of gratings having corrugations profiles with corners. Eqs. (22), (23) reveal that the previously demonstrated low asymptotic numerical complexity and memory consumption can be preserved in the new formulation, and the numerical examples show its importance in attaining accurate diffraction efficiencies. These results can be further utilized in the field of grating structure optimization, where computationally efficient and reliable rigorous solvers of the Maxwells equations are of great importance.

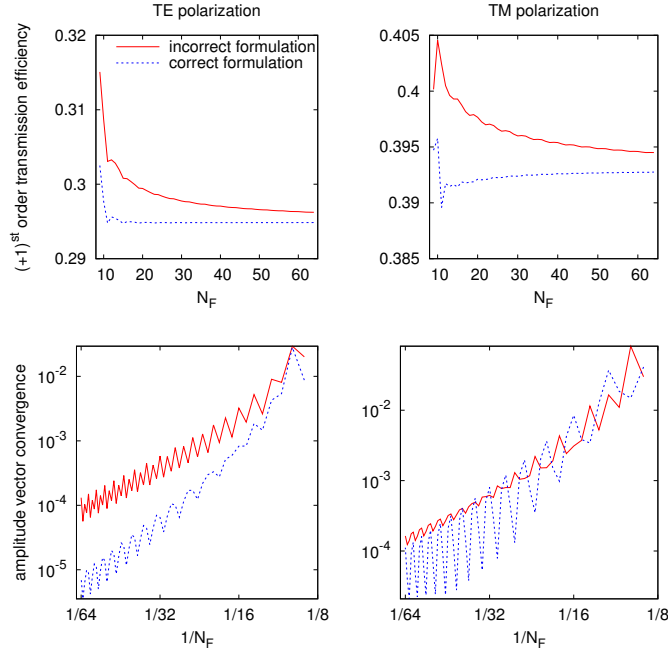


Figure 2: Convergence of the GSMCC in the previous formulation, which is incorrect for gratings having corrugation profile corners (red solid line), and in the present correct formulation (blue dashed line). The graphs are calculated for the grating depth-to-wavelength ratio $2a/\lambda = 0.5$, the period-to-wavelength ratio $\Lambda/\lambda = 1.5$, and the angle of incidence 10° . The number of slices is $N_s = 512$, permittivities of the covering medium and the grating are $\varepsilon_1 = 1$, $\varepsilon_2 = (2.5)^2$ respectively. The lower pair of graphs demonstrate the convergence of the central part of diffraction amplitude vector $\mathbf{a}^{e,out}$ corresponding to the lowest used number of Fourier harmonics.

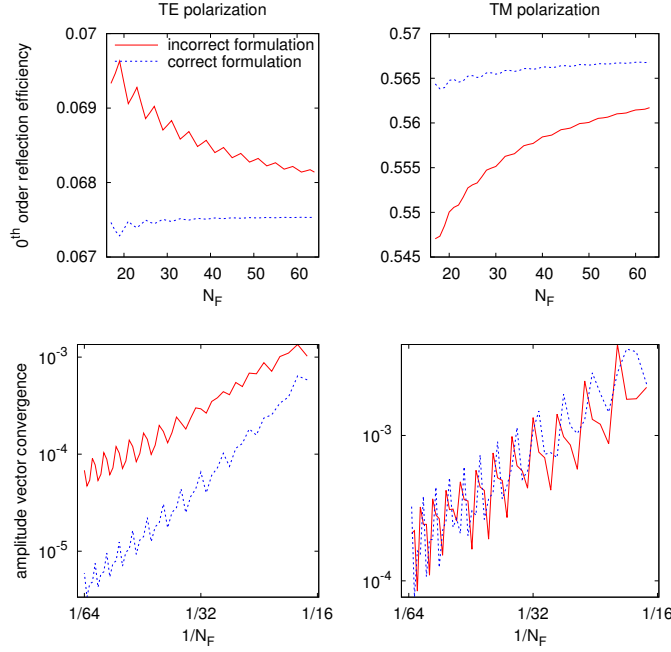


Figure 3: Same as in Fig. 2 but for metallic grating of permittivity $\varepsilon_2 = (0.2 + 3.2i)^2$.

Acknowledgments

The work was supported by the Russian Science Foundation, grant No. 17-79-20345.

Appendix

This appendix explicitly provides the matrices occurring in Eqs. (21)–(23). Indices k and l are used here to enumerate slices, and indices m and n are the Fourier indices. Transformation of Eqs. (19), (20) is given by the three matrices

$$N_{klmn} = \delta_{kl} \begin{pmatrix} \delta_{mn} & 0 & 0 \\ 0 & \mathcal{A}_{mn} & 0 \\ 0 & 0 & \mathcal{A}_{mn} \end{pmatrix}, \quad (24)$$

$$M_{klmn} = \delta_{kl} \begin{pmatrix} \delta_{mn} & 0 & 0 \\ 0 & \delta_{mn} + (\mathcal{B}\mathcal{B})_{mn} & 0 \\ 0 & 0 & \delta_{mn} + (\mathcal{B}\mathcal{B})_{mn} \end{pmatrix}, \quad (25)$$

$$\Omega_{klmn}^e = \delta_{kl} \begin{pmatrix} \eta_e \mathcal{A}_{mn} - \delta_{mn} & 0 & 0 \\ 0 & \eta_h \mathcal{A}_{mn} - \delta_{mn} - (\mathcal{B}\mathcal{B})_{mn} & (\mathcal{B}\mathcal{A})_{mn} \\ 0 & (\mathcal{B}\mathcal{A})_{mn} & \delta_{mn} + (\mathcal{B}\mathcal{B})_{mn} - \frac{1}{\eta_h} \mathcal{A}_{mn} \end{pmatrix}. \quad (26)$$

The terms $(\mathcal{BB})_{mn}$, and $(\mathcal{BA})_{mn}$ imply that vectors should be successively multiplied by the corresponding matrices. Block-diagonal matrices

$$\mathbf{P}_{klmn}^e = \delta_{kl}\delta_{mn} \begin{pmatrix} \frac{\omega\mu_b}{k_{m3}} & -1 & \frac{k_{m1}}{k_{m3}} \\ \frac{\omega\mu_b}{k_{m3}} & 1 & \frac{k_{m1}}{k_{m3}} \end{pmatrix}, \quad (27)$$

$$\mathbf{Q}_{klmn}^e = \delta_{kl}\delta_{mn} \begin{pmatrix} -1 & -1 \\ \frac{k_{m3}}{\omega\mu_b} & -\frac{k_{m3}}{\omega\mu_b} \\ -\frac{k_{m1}}{\omega\mu_b} & -\frac{k_{m1}}{\omega\mu_b} \end{pmatrix} \quad (28)$$

arise from the definition (4), and the scalar products in Eqs. (5), (7). Finally,

$$\mathbf{G}_{klmn} = -\delta_{mn} \frac{i\omega h_s}{2} \begin{pmatrix} \exp(ik_{m3}|z_k^3 - z_l^3|) & 0 \\ 0 & \exp(ik_{m3}|z_k^3 - z_l^3|) \end{pmatrix} \quad (29)$$

$$\mathbf{G}_{b,kmn} = -\delta_{mn} \frac{i\omega h_s}{2} \begin{pmatrix} \exp(ik_{m3}|b - z_k^3|) & 0 \\ 0 & \exp(ik_{m3}|z_k^3 + b|) \end{pmatrix} \quad (30)$$

in case when $\varepsilon_b = \varepsilon_1 = \varepsilon_2$. In general when the two permittivities $\varepsilon_{1,2}$ present in the regions $x_3 < -b$ and $x_3 > b$ are different from ε_b the Green's tensor becomes more complex, and the latter two matrix elements should be replaced with another ones incorporating multiple reflections at interfaces $x_3 = \pm b$. For explicit equations in this case see [25, 28].

In case of the TM polarization one has to interchange η_e and η_h in Eq. (26) to get Ω^h , and replace matrices ϵ^e , \mathbf{P}^e and \mathbf{Q}^e with

$$\epsilon_{mn,kl}^h = \delta_{mn}\delta_{kl} \text{diag} \{\mu_b, \varepsilon_b, \varepsilon_b\} \quad (31)$$

$$\mathbf{P}_{klmn}^h = \delta_{kl}\delta_{mn} \begin{pmatrix} \frac{\omega\varepsilon_b}{k_{m3}} & 1 & -\frac{k_{m1}}{k_{m3}} \\ \frac{\omega\varepsilon_b}{k_{m3}} & -1 & -\frac{k_{m1}}{k_{m3}} \end{pmatrix} \quad (32)$$

$$\mathbf{Q}_{klmn}^h = \delta_{kl}\delta_{mn} \begin{pmatrix} -1 & -1 \\ -\frac{k_{m3}}{\omega\varepsilon_b} & \frac{k_{m3}}{\omega\varepsilon_b} \\ \frac{k_{m1}}{\omega\varepsilon_b} & \frac{k_{m1}}{\omega\varepsilon_b} \end{pmatrix} \quad (33)$$

References

- [1] R. Petit, ed., *Electromagnetic Theory of Gratings*. Springer, 1980.
- [2] E. Popov, ed., *Gratings: Theory and Numeric Applications*. Institute Fresnel, AMU, 2012.
- [3] S. Molesky, L. Z., A. Y. Piggott, W. Jin, J. Vučković, and A. W. Rodriguez, "Inverse design in nanophotonics," *Nat. Photon.*, vol. 12, pp. 659–670, 2018.

- [4] L. Su, T. R., N. V. Saprà, A. Y. Piggott, S. Verduyck, and J. Vučković, “Fully-automated optimization of grating couplers,” *Opt. Expr.*, vol. 26, pp. 4023–4034, 2018.
- [5] P. Lalanne and G. M. Morris, “Highly improved convergence of the coupled-wave method for tm polarization,” *J. Opt. Soc. Am. A*, vol. 13, pp. 779–784, 1996.
- [6] G. Granet and B. Guizal, “Efficient implementation of the coupled-wave method for metallic lamellar gratings in tm polarization,” *J. Opt. Soc. Am. A*, vol. 13, pp. 1019–1023, 1996.
- [7] A. A. Shcherbakov and A. V. Tishchenko, “Fast numerical method for modeling one-dimensional diffraction gratings,” *Quant. Electron.*, vol. 40, pp. 538–544, 2010.
- [8] M. C. van Beurden, “Fast convergence with spectral volume integral equation for crossed block-shaped gratings with improved material interface conditions,” *J. Opt. Soc. Am. A*, vol. 28, pp. 2269–2278, 2011.
- [9] A. A. Shcherbakov and A. V. Tishchenko, “New fast and memory-sparing method for rigorous electromagnetic analysis of 2d periodic dielectric structures,” *J. Quant. Spectrosc. Radiat. Transf.*, vol. 113, pp. 158–171, 2012.
- [10] S. P. Skobelev and O. N. Smolnikova, “Analysis of doubly periodic inhomogeneous dielectric structures by a hybrid projective method,” *IEEE Trans. Antennas Propagat.*, vol. 61, pp. 5078–5087, 2013.
- [11] A. Junker and K.-H. Brenner, “Achieving a high mode count in the exact electromagnetic simulation of diffractive optical elements,” *J. Opt. Soc. Am. A*, vol. 35, pp. 377–385, 2018.
- [12] W. Iff, T. Kämpfe, Y. Jourlin, and A. Tishchenko, “Memory sparing, fast scattering formalism for rigorous diffraction modeling,” *J. Opt.*, vol. 19, p. 075602, 2017.
- [13] G. Granet, “Reformulation of the lamellar grating problem through the concept of adaptive spatial resolution,” *J. Opt. Soc. Am. A*, vol. 16, pp. 2510–2516, 1999.
- [14] G. Granet, J. Chandezon, J.-P. Plumey, and K. Raniriharinosy, “Reformulation of the coordinate transformation method through the concept of adaptive spatial resolution. application to trapezoidal gratings,” *J. Opt. Soc. Am. A*, vol. 18, pp. 2102–2108, 1999.
- [15] T. Weiss, G. Granet, N. A. Gippius, S.-G. Tikhodeev, and H. Giessen, “Matched coordinates and adaptive spatial resolution in the fourier modal method,” *Opt. Expr.*, vol. 17, pp. 8051–8061, 2009.
- [16] K. Edee and B. Guizal, “Modal method based on subsectional gegenbauer polynomial expansion for nonperiodic structures: complex coordinates implementation,” *J. Opt. Soc. Am. A*, vol. 30, pp. 631–639, 2013.
- [17] K. Edee, J.-P. Plumey, and B. Guizal, “Unified numerical formalism of modal methods in computational electromagnetics and the latest advances: Applications in plasmonics,” in *Advances in Imaging and Electron Physics*, vol. 197, ch. 2, pp. 45–103, 2016.

- [18] L. Li, “Use of fourier series in the analysis of discontinuous periodic structures,” *J. Opt. Soc. Am. A*, vol. 13, pp. 1870–1876, 1996.
- [19] E. Popov and M. Nevière, “Maxwell equations in fourier space: fast-converging formulation for diffraction by arbitrary shaped, periodic, anisotropic media,” *J. Opt. Soc. Am. A*, vol. 18, pp. 2886–2894, 2001.
- [20] B. Guizal, H. Yala, and D. Feldbacq, “Reformulation of the eigenvalue problem in the fourier modal method with spatial adaptive resolution,” *Opt. Lett.*, vol. 34, pp. 2790–2792, 2009.
- [21] J. Chandezon, D. Maystre, and G. Raoult, “A new theoretical method for diffraction gratings and its numerical application,” *J. Opt. (Paris)*, vol. 11, pp. 235–241, 1980.
- [22] G. Granet, “Analysis of diffraction by surface-relief crossed gratings with use of the chandezon method: application to multilayer crossed gratings,” *J. Opt. Soc. Am. A*, vol. 15, pp. 1121–1131, 1998.
- [23] X. Xu and L. Li, “Enlarging applicability domain of the c method with piecewise linear parameterization: gratings of deep and smooth profiles,” vol. 9526, p. 952605, SPIE Proceedings, 2015.
- [24] A. A. Shcherbakov and A. V. Tishchenko, “Efficient curvilinear coordinate method for grating diffraction simulation,” *Opt. Express*, vol. 21, pp. 25236–24247, 2013.
- [25] A. A. Shcherbakov and A. V. Tishchenko, “Generalized source method in curvilinear coordinates for 2D grating diffraction simulation,” *J. Quant. Spectrosc. Radiat. Transf.*, vol. 187, pp. 76–96, 2017.
- [26] A. A. Shcherbakov, Y. V. Stebunov, D. F. Baidin, T. Kämpfe, and Y. Jourlin, “Direct s-matrix calculation for diffractive structures and metasurfaces,” *Phys. Rev. E*, vol. 97, pp. 063301–10, 2018.
- [27] L. Tsang, J. A. Kong, and K.-H. Ding, *Scattering of electromagnetic waves: Theories and applications*. John Wiley & Sons, Inc., 2000.
- [28] L. C. Andreani and D. Gerace, “Photonic-crystal slabs with a triangular lattice of triangular holes investigated using a guided-mode expansion method,” *Phys. Rev. B*, vol. 73, p. 235114, 2006.
- [29] J. A. Schouten, *Tensor analysis for physicists*. Courier Corporation, 1989.
- [30] L. Li and J. Chandezon, “Improvement of the coordinate transformation method for surface-relief gratings with sharp edges,” *J. Opt. Soc. Am. A*, vol. 13, pp. 2247–2255, 1996.
- [31] J. D. Jackson, *Classical electrodynamics*. John Wiley & Sons, Inc., Third ed., 1993.